JCTC Journal of Chemical Theory and Computation

ARTICLE

pubs.acs.org/JCTC

Quantum Corrections to Classical Molecular Dynamics Simulations of Water and Ice

Qaiser Waheed* and Olle Edholm*

Department of Theoretical Physics, Royal Institute of Technology (KTH), AlbaNova University Center, SE-106 91 Stockholm, Sweden

ABSTRACT: Classical simulations of simple water models reproduce many properties of the liquid and ice but overestimate the heat capacity by about 65% at ordinary temperatures and much more for low temperature ice. This is due to the fact that the atomic vibrations are quantum mechanical. The application of harmonic quantum corrections to the molecular motion results in good heat capacities for the liquid and for ice at low temperatures but a successively growing positive deviation from experimental results for ice above 200 K that reaches 15% just below melting. We suggest that this deviation is due to the lack of quantum corrections to the anharmonic motions. For the liquid, the anharmonicities are even larger but also softer and thus in less need of quantum correction. Therefore, harmonic quantum corrections to the classically calculated liquid heat capacities result in agreement with the experimental values. The classical model underestimates the heat of melting by 15%, while the application of quantum corrections produces fair agreement. On the other hand, the heat of vaporization is overestimated by 10% in the harmonically corrected classical model.

1. INTRODUCTION

Structural and thermodynamic properties of water have been extensively studied with classical molecular dynamics simulations using three site models like the simple point charge (SPC) model,[1] the slightly modified SPC/E model,[2] or the TIP3P[3] model. In general, these models describe many equilibrium properties of the liquid as well as or better than models involving more than three interaction sites. There is a remarkable exception; slight reparametrizations of the classical four-site model (TIP4P[3]) have produced a couple of models, TIP4P/2005[4] and TIP4PQ/2005,[5] which reproduce ice and liquid properties including many temperature dependencies much better than the three-site models. Even, compared to much more time-consuming computer simulation methods, like Car−Parrinello molecular dynamics[6] (CPMD), which calculates the forces on the atoms directly from electron structure calculations performed at each time step, these classical models behave quite well.

There is, however, one important exception. None of these models (including the CPMD one) give reasonable heat capacities. In their original versions, the classical models have fixed bond lengths and bond angles. These degrees of freedom can be made flexible, but this will not improve results but rather make them worse since the bond length and angle potentials are stiff enough to make a quantum mechanical treatment necessary. Further, the vibration of the entire molecules in ice as well as liquid water is also quantum mechanical. Therefore, a simple classical model or even one that treats the electrons but not the nuclei by quantum mechanics is insufficient for this purpose. There is one simple way around this problem that was suggested and tried out successfully on liquid water by Berens et al.[7] in 1983. If one assumes that the vibrational motion is harmonic, one may calculate a correction to the classical heat capacity from the difference between that of a quantum and that of a classical oscillator. One, just has to integrate over all frequencies with the weight taken from the normal mode spectrum. For liquid water, this reduces the difference compared to experiment from 45% to 4%.[7] These kinds of methods are not limited to water but may be applied to much more complex systems. They have, however, since then only been applied to a few other systems. Liquid methanol[8] and solid argon[9] are two examples.

An alternative technique, path integral molecular dynamics/Monte Carlo (PIMD/PIMC), should in principle be able to produce correct heat capacities since it handles the nuclei quantum mechanically and avoids the harmonic approximation. The sparse results[5,10−13] are promising, despite some differences and that some fine-tuning of the potential parameters with respect to their classical values seems to be required.

Here, we have applied the original harmonic correction method to ordinary ice (I_h) using the SPC/E model. In this case, quantum effects are even larger than in liquid water. Bond lengths and the bond angle have been fixed as in the original SPC/E model since these degrees of freedom are rigid enough to give negligible contributions to the heat capacity. The energy fluctuations were used to calculate the classical heat capacities (see, e.g., a textbook like Allen and Tildesly[14]), while the normal mode density was calculated from the velocity autocorrelation functions.

2. THEORY

The heat capacity at constant volume, C_V, of a classical system can be calculated from the fluctuations in energy, σ_E, in a simulation at conserved volume, temperature, and particle number (NVT) as

$$C_V = \sigma_E^2/k_B T^2 \quad (1)$$

Received: May 2, 2011
Published: August 03, 2011

with k_B being the Boltzmann constant and T the absolute temperature. Alternatively, it may be obtained as a numerical derivative of the total energy with respect to the temperature. The heat capacity at constant pressure, C_p, can be obtained from the enthalpy fluctuations, σ_H, in a simulation at fixed pressure (NpT) as

$$C_p = \sigma_H^2/k_B T^2 = (\sigma_E + p\sigma_V)^2/k_B T^2 \quad (2)$$

See, e.g., refs 14 and 15 for the background. We have chosen to do the simulations at fixed volume, which gives the C_V's. Experimental heat capacities are, however, more often available as C_p's. For condensed matter systems, the difference is small, and the two types of heat capacities can readily be converted between each other using the exact thermodynamic relation (see e.g., ref 16):

$$C_p - C_V = VTK_V\alpha^2 \quad (3)$$

where the thermal expansion coefficient, $\alpha = 1/V(\partial V/\partial T)_p$, and volume compressibility modulus, $K_V = -V(\partial p/\partial V)_T$, are experimentally available. Thus, experimental C_p's can be converted into C_V's by employing this relation. The difference between the two types of heat capacities is less than 1% in the condensed water phases.

Quantum corrections to the classical heat capacities cannot easily be calculated in general without employing models or approximations. One fairly good and practical model is that of coupled harmonic oscillators, which gives an analytically solvable problem. Transformation to normal coordinates gives decoupled harmonic oscillators. The contribution of each such oscillator to the heat capacity is then

$$k_B\left(\frac{\hbar\omega}{k_B T}\right)^2 \frac{\exp(\hbar\omega/k_B T)}{[\exp(\hbar\omega/k_B T) - 1]^2} \quad (4)$$

This depends on the angular frequency, ω, of the oscillator through the dimensionless energy $x = \hbar\omega/k_B T$ (with $\hbar$ being Planck's constant divided by 2π). In the classical limit (small x or large T), we regain the Dulong–Petit result, k_B per degree of freedom. In the other (quantum) limit, the contribution to the heat capacity goes to zero. Thus, knowing the angular frequencies, ω_i ($x_i = \hbar\omega_i/k_B T$), of the normal modes, the quantum correction to the classical heat capacity per molecule is obtained as

$$\Delta c_V = k_B \sum_i \left[x_i^2 \frac{e^{x_i}}{(e^{x_i} - 1)^2} - 1\right] \approx k_B \int_0^\infty \left[x^2 \frac{e^x}{(e^x - 1)^2} - 1\right] G(x)\, dx \quad (5)$$

In the integral approximation, the integral is performed over the dimensionless variable x. The normal mode distribution, $g(\omega)$, is normalized to give the integral $\int g(\omega)\, d\omega$, equal to the number of degrees of freedom per molecule, i.e., 6 for rigid water and 9 for flexible water. As a function of the dimensionless variable x, the normal mode distribution $G(x)$ is equal to $(k_B T/\hbar)\, g(k_B T x/\hbar)$. The normal mode distribution may be obtained from the velocity spectrum as[7,15]

$$g(\omega) = N \frac{\sum_i |\hat{v}_i(\omega)|^2}{\int \sum_i |\hat{v}_i(\omega)|^2 d\omega} \quad (6)$$

were $\hat{v}_i(\omega)$ is the Fourier transform of an atomic velocity component, the sum goes over all three components of all atoms, and N is the number of degrees of freedom (6 or 9 per molecule).

The quantum corrections are negative and thus reduce the heat capacities. The SPC/E water model used here has point charges at the positions of the oxygen and the two hydrogens and Lennard-Jones interactions between the oxygens. It is usually simulated with fixed bond lengths and a fixed bond angle, but one may also perform classical simulations with harmonic vibrations in the bonds and the angle. The angular frequencies of these oscillators correspond, however, to large values of $x = \hbar\omega/k_B T$ (about 7 for the angle and 14 for the bonds at 300 K). Thus, the contribution from these degrees of freedom becomes negligible after application of quantum corrections (about $0.04k_B$ per molecule compared to the classical value $3k_B$)

The quantum correction to the energy may also be calculated as

$$\Delta u_{QM} = k_B T \int_0^\infty \left(\frac{x}{2} + \frac{x}{e^x - 1} - 1\right) G(x)\, dx = u_0 + u_e - u_{cl} \quad (7)$$

The first term, u_0, is the ground state energy of the harmonic oscillators, u_e the energy in the excited states, while u_{cl} is the classical energy (6 or 9 $k_B T$). The melting enthalpy of ice and the heat of vaporization of liquid water could thus be quantum corrected. The melting enthalpy of ice is

$$\Delta H = H_l - H_s = (U_l + pV_l) - (U_s + pV_s) = \Delta U + p\Delta V \quad (8)$$

with the $p\Delta V$ term being negligible (-1.6×10^{-4} kJ/mol) compared to ΔU (6 kJ/mol).

3. COMPUTATIONAL DETAILS

All simulations were performed using the GROMACS[17] package, version 4.0, on a local cluster in the department at Albanova University Center KTH Stockholm. All systems consisted of 360 SPC/E water molecules and were subjected to periodic boundary conditions in all directions. Liquid water was simulated at 300 K and 273 K, while ice was simulated at the temperatures of 273, 263, 243, 223, 173, 93, and 23 K. A Nose–Hoover thermostat[18,19] was used to keep the temperature constant for the system. The integration of the equations of motion was performed by using a leapfrog algorithm with a time step of 1 fs. Liquid water was simulated with fixed as well as flexible bonds and angles, but the main part of the ice simulations was done with rigid water molecules. During the equilibrations, a barostat was used to adjust the density to obtain a pressure of 1 bar. The simulations used to calculate energy fluctuations and normal mode distributions were performed at a fixed volume and temperature (NVT). The analytical SETTLE algorithm[20] was used to restrain bond lengths and angles. In simulations with flexible bonds and angles, a test with a 10-fold reduced time step did not alter any results. The classical heat capacity was calculated from the energy fluctuations over 5 ns simulations which had been equilibrated for 1 ns, while the normal mode distributions were calculated from the velocities in densely stored 500 ps trajectories. A cutoff of 1.0 nm was used for Lennard-Jones (LJ) interactions. The electrostatics were calculated using the particle-mesh Ewald (PME) method[21,22] with interactions inside 1.0 nm

Table 1. c_V's of Liquid Water and Ice Calculated from Experimental c_p's[24] Using eq 3 with Experimental Thermal Expansion Coefficients and Compressibility Modulii[23]

phase	l		s						
T [K]	300	273	273	263	243	223	173	93	23
c_V [J/mol K]	74.1	74.8	37.0	35.6	33.1	30.4	24.3	14.9	3.1
c_p [J/mol K]	75.2	75.9	38.0	36.5	33.8	31.0	24.5	14.9	3.1

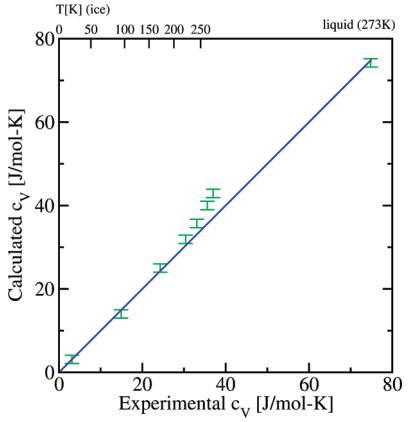

Figure 1. Calculated versus experimental heat capacities at different temperatures. The simulation figures are given with an error bar of 1 J/mol·K. The straight line ($y = x$) indicates perfect agreement.

handled in real space and those outside in Fourier space. For water and ice, the SPC/E model[1,2] was used.

4. RESULTS AND DISCUSSION

The experimental c_p's[24] are shown in the Table 1 together with the c_V's calculated using eq 3 with experimental values[23] for α and K_V. Alternatively, c_p's could be obtained by converting the c_V's from the simulations using eq 3. For this, α and K_V were determined from ice simulations at 273 K as 260×10^{-6} K^{-1} and 0.23×10^{10} N/m^2. These values deviate substantially from the experimental ones but give only a slightly lower difference of 0.8 J/mol·K instead of 1.0 J/mol·K between the heat capacities.

The heat capacities obtained after applying quantum corrections to the classical simulation data are shown versus the experimental ones in Figure 1 and in Table 2 with the quantum corrections tabulated separately. For liquid water, the rigid SPC/E model[1,2] gives an as-good (or even marginally better) heat capacity as the more complicated flexible Watts model[27] used by Berens et al.[7] The usage of flexible bonds and bond angles in the SPC/E model gives, on the contrary, a substantial overestimate of the heat capacity. The reason for this is that almost twice the energy expected from equipartition goes into these degrees of freedom. This was observed already in 1991 by Wallqvist and Teleman.[28] The deviation from equipartition decreases at lower densities and higher temperatures. We decided to stick to the rigid water model in the ice simulations. The ice simulations showed good agreement for the heat capacity at low temperatures, while the heat capacity was overestimated by about 15% (5−6 J/mol·K), close to the melting point. The classical heat capacities in Table 2 obtained from energy fluctuations were checked by numerical differentiation of the total energies

Table 2. Calculated (Classical and Quantum Corrected) and Experimental (from Table 1) Heat Capacities in J/mol·K for Liquid Water and Ice at Different Temperatures[a]

T	class c_V	QM corr.	corr. c_V	exptl. c_V
300 K (l), flex.	122.9 ± 1.4	−37.1	85.8	74.1
300 K (l), rigid	86.6 ± 0.7	−14.4	72.2	74.1
273 K (l), rigid	88.8 ± 0.7	−14.6	74.2	74.8
273 K (s)	62.2 ± 0.3	−19.3	42.9	37.0
263 K (s)	60.5 ± 0.3	−20.5	40.0	35.6
243 K (s)	58.2 ± 0.3	−22.5	35.7	33.1
223 K (s)	56.3 ± 0.3	−24.4	31.9	30.4
173 K (s)	53.9 ± 0.5	−28.9	25.0	24.3
93 K (s)	52.0 ± 0.3	−38.0	14.0	14.9
23 K (s)	50.0 ± 0.4	−47.0	3.0	3.1

[a] The total statistical error is estimated to be around ±1 J/mol·K from the statistical error in column 2 and an error in the quantum correction of ±0.5 J/mol·K due to insufficient sampling of the normal mode distribution.

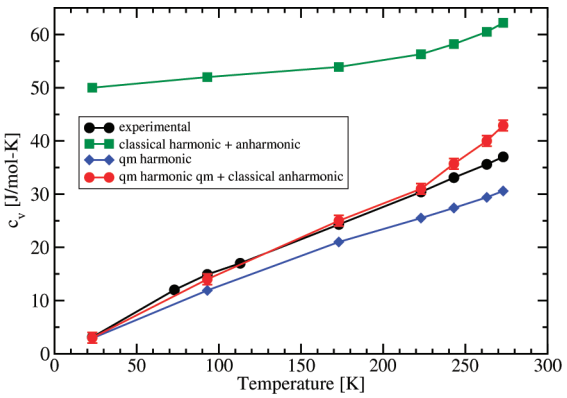

Figure 2. Experimental and calculated heat capacities versus temperature. The calculated heat capacities are (i) the classical ones containing harmonic as well as anharmonic contributions, (ii) the heat capacity from quantum mechanical harmonic oscillators, and (iii) the classical heat capacity with the harmonic part quantum-corrected.

showing no significant differences. We also checked that the larger heat capacities in ice close to the melting temperature were not due to critical fluctuations. Varying the system size (up and down) showed that the fluctuations in total energy scaled as would be expected from eq 1 ($\sigma_E \propto (N)^{1/2}$). The difference close to melting can therefore not be attributed to critical fluctuations. We also checked the sensitivity of the normal mode distribution to system size and found none.

In the Figure 2, the experimental and calculated heat capacities of ice are plotted versus the temperature. The experimental ones fit a straight line starting at zero for $T = 0$ with a slight deviation upward around 100 K. The QM corrected simulation data agree with experimental; results up to about 200 K, including the upward deviation from the straight line. At higher temperatures, the calculated heat capacities deviate upward in a way that could be described by a quadratic correction. The classical heat capacity calculated from the energy fluctuations is also shown. This is 20−50 J/mol·K larger than the experimental one, approaches the constant Dulong−Petit value, $6k_B$ = 49.9 J/mol·K at low temperatures, but is about 13 J/mol·K higher close to melting.

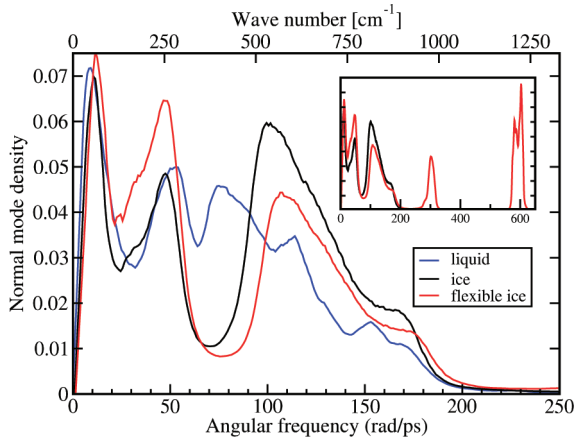

Figure 3. The normal mode distributions of ice and liquid water at 273 K with fixed bond lengths and bond angles. The normal mode distribution for ice with flexible bond lengths and angles is also shown. The inset includes the high frequency bond length and bond angle vibrations.

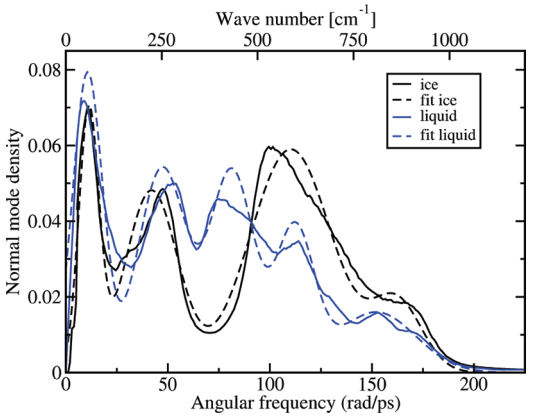

Figure 4. The normal mode distributions of ice and water at 273 K together with fits to 4 and 5 Gaussians, respectively.

This indicates that anharmonicities play an increasing role with temperature. It is, however, reassuring that experimental and calculated quantum corrected heat capacities agree at low temperatures when anharmonic contributions are expected to be small. Alternatively, one may apply a pure quantum harmonic oscillator model with the angular frequencies taken from the classical normal-mode analysis.

The heat capacities resulting from this model are also shown in Figure 2. It it clear that this model substantially underestimates the heat capacity except for very low temperatures (at which the anharmonic contribution is negligible). The quantum-corrected classical result could alternatively be viewed as the superposition of this result with the classical anharmonic contribution. This clearly reduces the error compared to when the anharmonic contribution is entirely neglected. For the highest temperatures, it does, however, overestimate the heat capacity since it misses the quantum corrections to the anharmonic contribution, which certainly would reduce the heat capacity if they could be included properly. In the liquid, the calculated heat capacity is, on the contrary, slightly on the low side, although almost within the statistical accuracy. Still, the deviation from the Dulong−Petits law is substantially larger in the liquid, indicating large anharmonic contributions to the heat capacity. These are, however, softer and thus more or less classical.

PIMD/MC methods[5,10−13] give the heat capacity without resorting to harmonic approximations. A recent study[29] employing a slightly reparametrized TIP4P/2005 model (TIP4PQ/2005) produces excellent agreement for the temperature-dependent heat capacity of ice as well as liquid water. Some of the earlier studies show less good results. The reason for that may be either that the underlying classical model is not good enough or that the fairly time-consuming simulations have not been performed long enough to produce adequate sampling.

The calculated normal mode distributions are shown in Figures 3−5. Figure 3 shows the normal mode distributions of the liquid and solid at 273 K. For ice, four broad peaks can be resolved at the angular frequencies in rad/ps or (THz) at 10(1.6), 50(8.0), 100(16), and 170(27) (corresponding to 53, 265, 530, and 900 cm^{-1} in spectroscopic units). For liquid water, the two lowest peaks are well resolved with just slight position shifts compared to ice. The pronounced minimum in the normal mode distribution of ice at 75 rad/ps is absent in the liquid, and the two broad peaks at higher frequencies are replaced by a broader distribution. Both densities of state drop to zero just above 200 rad/ps. The normal mode distribution of ice may be compared to the experimental density of states obtained from neutron scattering.[25] The pronounced minimum between 75 and 100 rad/ps in the simulated distribution agrees with a similar minimum in the experimental distribution. Otherwise, the spectra are qualitatively similar. The difference between the densities of state of H_2O and D_2O shows[26] clearly that the high-ω part of the spectrum (above the minimum) is due to rotational vibrations, while the lower part is due to translational vibrations. We verified this in simulations by increasing the mass of the hydrogens to 4 and reducing the oxygen mass to 8. Thus, the total mass of the molecule remained constant, which should result in an unaltered translational part of the spectrum. On the contrary, the rotational part should move down a factor 2 due to the 4-fold increase of the moment of inertia. We did observe (not shown) an essentially unaltered low-ω part of the density of states, while the part above 75 rad/ps was shifted down by a factor 2.

The fairly linear variation of the heat capacity with temperature shown in Figure 2 results from the broad distribution of oscillator frequencies but also from the fact that a single quantum oscillator (see eq 4) has a smooth variation of the heat capacity with the temperature. The heat capacity is half its classical value at the temperature $T_{1/2} \equiv \hbar\omega/3k_B$, with the change from 10% to 90% occurring in the fairly broad temperature interval $(0.5-3)T_{1/2}$. With the peaks in the normal mode density at frequencies corresponding to $T_{1/2}$ of 25, 120, 260, and 410 K, a considerable overlap in variation is obtained, resulting in a smooth variation of the heat capacity, which turns out to be fairly linear.

Figure 4 shows that a small number of Gaussians fit the normal mode distributions quite well. For ice, a decent fit is obtained using four Gaussians, while the liquid needs five, which still do not agree as well. Finally, the normal mode distributions of ice obtained at different temperatures are shown in Figure 5. There are fairly small but clear differences, and the distribution is shifted toward higher frequencies with more pronounced peaks at lower temperatures. This indicates that there are anharmonic parts in the potential which come out differently in normal mode distribution derived from the velocity autocorrelations at different temperatures. Still, the difference is small enough to have just minor effects on the quantum corrections. The quantum correction calculated at 273 K

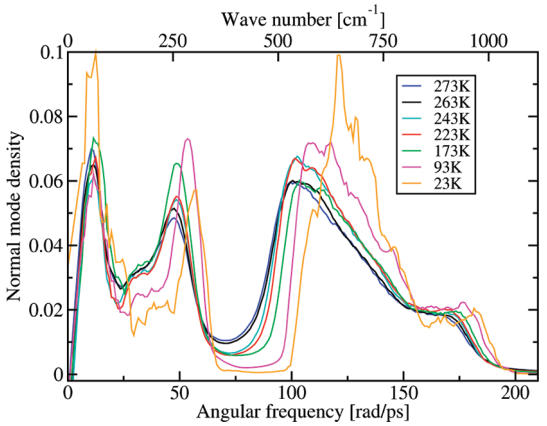

Figure 5. The calculated normal mode distributions for ice at different temperatures.

Table 3. Frequencies, ν, of the Internal Bending and Stretching (Symmetric (s) and Asymmetric (a)) Modes of Water in Different Phases in the Spectroscopic Unit, cm^{-1}[a]

	phase	bending	stretching (s)	stretching (a)
calculated	g	1592	3184	3243
experiment	g	1595	3657	3756
simulations	l	1610	3130	3220
experiment	l	1645	3280	3490
simulations	s	1600	3090	3200
experiment	s	1650	3085	3220

[a] The experimental values are based on IR and Raman spectra and are taken from refs 30 and 34 for the gas phase, from ref 23 for the liquid, and from refs 35 and 36 for the ice. The calculated values for the gas phase were obtained analytically (see, e.g., ref 32) from the geometry and force constants of the flexible SPC/E water model. The simulation values for the condensed phases were obtained from the normal mode distribution of flexible water.

from the density of states taken from the 23 K simulation is −19.8 instead of −19.3 J/mol·K as obtained with the proper distribution.

The inset in Figure 3 shows the normal mode distribution of ice with flexible and rigid molecules. In the flexible model, the angle vibrations show up as a narrow peak at 300 rad/s, while there are two overlapping peaks close to 600 rad/ps due to bond length vibrations. The area under the angle peak is approximately 1, while that under the double stretching peak deviates slightly from 2. This deviation indicates a slight mixing with the soft degrees of freedom, which is further substantiated by small differences in the low frequency part of the normal mode spectra. Table 3 shows the angular frequencies of the internal vibrational modes of water molecules in different phases as obtained from simulations using standard flexible SPC/E water. They are compared to spectroscopically determined angular frequencies in the liquid and gas phases. It is clear that the large experimental downward shift and broadening of the stretching peaks in the condensed phases are only partially reproduced in classical simulations. The standard choices of angular frequency for the bond stretching and bond angle vibrations used in the classical SPC and SPC/E water models are 3.45×10^8 J/mol nm^2 and 3.83×10^5 J/mol rad^2. As seen from Table 3, this reproduces the

Table 4. Total Classical Energies (Kinetic Plus Potential) and Harmonic Quantum Corrections for Ice, Liquid Water, and Water Vapor at 273 K[a]

energy [kJ/mol]	U_s	U_l	U_g	$U_l - U_s$	$U_g - U_l$
		intermolecular			
classical rigid model	−46.48	−41.40	6.81	5.08	48.21
QM corr.:$u_0 + u_e - u_{cl}$	6.85	5.35	0.0	−1.50	−5.35
		intramolecular			
QM ground state	47.59	50.34	53.89	2.75	3.55
quantum corrected	7.96	14.29	60.70	6.33	46.41

[a] The quantum corrections were calculated from eq 7 using the normal mode distributions in Figure 3 for the intermolecular part, while experimental bending and stretching frequencies (Table 3) were used for the intramolecular ground state energy (the excited states give negligible contributions).

experimental frequencies in the condensed phases and especially the solid phase better than those of the gas phase. The TIP3P and TIP4P water models use a slightly more stiff bond and bond angle.

The heats of melting and vaporization are easily calculated from the energy differences between the different phases. To obtain accurate values, one may have to apply quantum corrections as discussed for the liquid by Burnham and Xantheas.[37] In Table 4, we give the total energies from simulations of rigid solid and liquid water at 273 K. For the gas, we just have $3k_BT$ of kinetic energy and need no simulation. Both ice and liquid water are stable in very long time simulations at this temperature, even if the actual solid/liquid transition temperature may be different from the experimental one for the present (and other) water models. The classical intermolecular energy is now corrected by calculating the three terms in eq 7 from the normal mode distributions from Figure 3. The correction consists of two parts. The normal mode spectrum of the ice is shifted toward higher angular frequencies, which gives rise to a higher zero point energy in ice, but also to a lower average energy in the excited states in ice. The net effect from the intermolecular part will be a change of the melting enthalpy by −1.50 kJ/mol. The internal vibrational frequencies contribute through different zero point energies, smaller for ice and larger for liquid water. This gives using the experimental vibrational frequencies an additional correction of +2.75 kJ/mol to the heat of melting. When the total quantum correction, 1.25 kJ/mol, is added to the classically calculated heat of melting, 5.08 kJ/mol, a heat of melting of 6.33 kJ/mol is obtained in good agreement with experimental value of 6.01 kJ/mol.[33] The total quantum correction is smaller here than the value suggested in ref 37 of 2.75 kJ/mol. The reason for this is that we use different normal mode distributions for the intermolecular degrees of ice and liquid water (calculated from respective simulations), while Burnham and Xantheas[37] used the same normal mode distribution. For the intramolecular part, we use the same experimental vibration frequencies as they and thus have identical results. The classical TIP4P/2005 model has an energy of −49.52 kJ/mol for the liquid at 273 K,[38] while the corresponding energy for the I_h-ice is −55.84 kJ/mol at 250 K. From the latter value, we obtain −54.41 kJ/mol at 273 K using the heat capacity of classical ice (with restrained bond lengths and bond angles), 62.00 J/mol·K. Thus, this model gives the classical heat of melting, 4.89 kJ/mol. If we assume the same

quantum corrections as for the SPC/E model, we obtain 6.14 kJ/mol in slightly better agreement with experimental results.

To explore the quality of the water model and the correction scheme further, we may also calculate harmonic quantum corrections to the heat of vaporization. Originally, the classical potential energy was used to adjust the parameters of, for instance, the SPC model[1] to obtain the correct heat of vaporization. Since then, lattice summations methods for the electrostatics (instead of short cutoffs), dispersion corrections for the Lennard-Jones interactions, and other adjustments have been introduced. There are two quantum effects. First, the intermolecular energy of the liquid increases by 5.35 kJ/mol (see Table 4) as a net result of zero point energy and smaller energy in the excited states. Second, Table 3 shows that the experimental vibrational frequencies of the bond lengths are substantially larger in the gas phase compared to the liquid phase. Thus, the quantum mechanical ground state energy of the internal degrees of freedom is larger in the gas phase. On the basis of the experimental figures, we get 3.55 kJ/mol. This goes in the opposite direction of the correction to the intermolecular potential energy, and the net reduction of the heat of vaporization becomes 1.80 kJ/mol. From the quantum corrected difference in energy between the gas and the liquid, 46.41 kJ/mol, we obtain after adding the *RT* term the heat of vaporization, 48.69 kJ/mol (at 273 K). This is clearly larger than the experimental value, 45.05 kJ/mol.[33] One may note that the original SPC model, which was parametrized against the heat of vaporization, produces better agreement due to its 3.4% smaller charges. The SPC/E model has, however, other advantages. For the TIP4P/2005 model, the energy of the liquid at 273 K (see above[38]) results in a heat of vaporization (51.78 kJ/mol) which with the same quantum correction becomes 49.98 kJ/mol. The TIP4PQ/2005 model, which has 3.6% larger charges, has an even more negative energy[39] resulting in a heat of vaporization around 56.2 kJ/mol after the same quantum corrections. Different PIMD/MC studies[12,13,39] indicate a difference in energy between PIMD/PIMC and classical simulations of 4−7 kJ/mol in the liquid state. The present quantum correction to the intermolecular energy, 5.35 kJ/mol, agrees favorably with this value. It is not obvious how the different intramolecular zero-point energies of the liquid and the gas are handled in the PIMD/MC simulations. Either similar corrections to those here could be applied or flexible molecules with different force constants in the different phases could be simulated. We conclude that the SPC/E as well as the TIP4P/2005 and TIP4PQ/2005 models have on the order 10% too strong cohesive interactions to reproduce experimental heats of vaporization, while the original SPC model seems to give better agreement. Although the difference is noteworthy, we do not think that this is a serious problem for the water models.

5. CONCLUSION

Simple classical rigid three-atom models for liquid water like the SPC/E model used here (or the SPC and TIP3P models) have essentially three parameters, the dipole moment (given by the charge separation between the oxygen and hydrogens) and the two Lennard-Jones parameters. The geometry of the molecule, given by the bond length and bond angle does not leave much room for variation. Thus, these three parameters can be determined to reproduce three different properties at one given density and temperature. Still such simple models reproduce several other properties of the liquid reasonably well and also give stable ice at lower temperatures. We have shown here that even the temperature-dependent heat capacity of the ice can be reasonably reproduced after the application of quantum corrections. There is, however, still a 15% error in the heat capacity of ice close to melting that most likely is due to quantum mechanical anharmonicities. The heat of melting, which in the classical approximation is underestimated by about 15%, is on the other hand obtained very close to the experimental value after the application of quantum corrections to the SPC/E as well as the TIP4P/2005 models. The heat of vaporization is on the other hand overestimated by about 10%, even after application of the relatively small quantum corrections.

AUTHOR INFORMATION

Corresponding Author

*Phone:+46-8-55378168. E-mail: qasir2@kth.se; oed@kth.se.

ACKNOWLEDGMENT

We thank professor Göran Grimvall for helpful discussions and suggestions concerning the interpretation of the normal mode spectra of ice. Q.W. acknowledges support by a grant from the Higher Education Commission (HEC) Pakistan. O.E. acknowledges the support by a grant from the Swedish Research Council (VR).

REFERENCES

(1) Berendsen, H. J. C.; Postma, J. P. M; van Gunsteren, W. F.; Hermans, J. Interaction models for water in relation to protein hydration. In *Intermolecular Forces*; Pullman, B., Ed.; D. Reidel Publishing Company: Dordrecht, Netherlands, 1981; pp 331−342.

(2) Berendsen, H. J. C.; Grigera, J. R.; Straatsma, T. P. *J. Phys. Chem.* **1987**, *91*, 6269.

(3) Jorgensen, W. L.; Chandrasekhar, J.; Madura, J. D.; Impey, R. W.; Klein, M. L. *J. Chem. Phys.* **1983**, *79*, 926.

(4) Abascal, J. L. F.; Vega, C. *J. Chem. Phys.* **2005**, *123*, 234505.

(5) McBride, C.; Vega, C.; Noya, E. G.; Ramirez, R.; Sesé, L. M. *J. Chem. Phys.* **2009**, *131*, 024506.

(6) Marx, D.; Hutter, J. Getting started: unifying MD and electronic structure. In *Ab Initio Molecular Dynamics*; Cambridge University Press: New York, 2009; pp 27−50.

(7) Berens, P. H.; Mackay, D. H. J.; White, G. M.; Wilson, K. R. *J. Chem. Phys.* **1983**, *79*, 2375.

(8) Hawlicka, E.; Pálinkás, G.; Heinzinger, K. *Chem. Phys. Lett.* **1989**, *154*, 255.

(9) Hardy, R. J.; Lacks, D. J.; Shukla, R. C. *Phys. Rev. B* **1998**, *57*, 833.

(10) Stern, H. A.; Berne, B. J. *J. Chem. Phys.* **2001**, *115*, 7622.

(11) Shinoda, W.; Shiga, M. *Phys. Rev. E.* **2005**, *71*, 041204.

(12) Shiga, M.; Shinoda, W. *J. Chem. Phys.* **2005**, *123*, 134502.

(13) Donchev, A. G.; Galkin, N. G.; Illarionov, A. A.; Khoruzhii, O. V.; Olevanov, M. A.; Ozrin, V. D.; Subbotin, M. V.; Tarasov, V. I. *Proc. Natl. Acad. Sci U. S. A.* **2006**, *103*, 8613.

(14) Allen, M. P.; Tildesley, D. J. Statistical mechanics. In *Computer Simulation of Liquids*; Oxford University Press: New York, 1986; pp 65−68.

(15) McQuarrie, D. A. In *Statistical Mechanics*; Harper Collins Publishers: New York, 1976.

(16) Plischke, M.; Bergersen, B. In *Equilibrium Statistical Physics*, 3rd ed; World Scientific: Singapore, 1994.

(17) van der Spoel, D.; Lindahl, E.; Hess, B.; Groenhof, G.; Mark, A. E.; Berendsen, H. J. C. *J. Comput. Chem.* **2005**, *26*, 1701.

(18) Nosé, S. *Mol. Phys.* **1984**, *52*, 255.

(19) Hoover, W. G. *Phys. Rev. A.* **1985**, *31*, 1695.

(20) Miyamoto, S.; Kollman, P. A. *J. Comput. Chem.* **1992**, *13*, 952.
(21) Darden, T.; York, D.; Pedersen, L. *J. Chem. Phys.* **1993**, *98*, 10089.
(22) Essmann, U.; Perera, L.; Berkowitz, M. L.; Darden, T.; Lee, H.; Pedersen, L. G. *J. Chem. Phys.* **1995**, *103*, 8577.
(23) Eisenberg, D.; Kauzmann, W. In *The Structure and Properties of Water*; Oxford University Press: Oxford, U. K., 1969.
(24) Nhemethy, G.; Scheraga, H. A. *J. Chem. Phys.* **1962**, *36*, 3382.
(25) Li, J. C.; Londono, J. D.; Ross, D. K.; Finney, J. L.; Tomkinson, J.; Sherman, W. F. *J. Chem. Phys.* **1991**, *94*, 6770.
(26) Criado, A.; Bermejo, F. J.; Garcia-Hernandez, M.; Martinez, J. L. *Phys. Rev. E.* **1993**, *47*, 3516.
(27) Watts, R. O. *Chem. Phys.* **1977**, *26*, 367.
(28) Wallqvist, A.; Teleman, O. *Mol. Phys.* **1991**, *74*, 515.
(29) Vega, C.; Conde, M. M.; McBride, C.; Abascal, J. L. F.; Noya, E. G.; Ramirez, R.; Sesé, L. M. *J. Chem. Phys.* **2010**, *132*, 046101.
(30) Herzberg, G.; In *Molecular Spectra and Molecular Structure. II. Infrared and Raman Spectra of Polyatomic Molcules*; Van Nostrand: Princeton, NJ, 1945.
(31) Walrafan, G. E. In *Water, a Comprehensive Treatise, The Physics and Chemistry of Water*; Franks, F., Eds.; Plenum: New York, 1972; Vol 1, p 151.
(32) Landau, L. D.; Lifshitz, E. M. In *Mechanics*; Pergamon Press: London, 1976.
(33) Lide, D. R. In *CRC Handbook of Chemistry and Physics*, 88th ed.; CRC Press: Boca Raton, FL, 2008.
(34) Benedict, W. S.; Plyler, E. K.; Gailar, N. *J. Chem. Phys.* **1956**, *24*, 1139.
(35) Bertei, J. E.; Whalley, E. *J. Chem. Phys.* **1964**, *40*, 1637.
(36) Taylor, M. J.; Whalley, E. *J. Chem. Phys.* **1964**, *40*, 1660.
(37) Burnham, C. J; Xantheas, S. S. *J. Mol. Liq.* **2004**, *110*, 177.
(38) Pi, H. L.; Aragones, J. L.; Vega, C.; Noya, E. G.; Abascal, J. L. F.; Gonzalez, M. A.; McBride, C. *Mol. Phys.* **2009**, *107*, 365.
(39) Noya, E. G.; Vega, C.; Sesé, L. M.; Ramirez, R. *J. Chem. Phys.* **2009**, *131*, 124518.